On the influence of surface quenching, electron emission and surface recombination on discharge properties

Jón Tómas Guðmundsson[1,2]

[1] Science Institute, University of Iceland, Reykjavik, Iceland
[2]Department of Space and Plasma Physics, KTH Royal Institute of Technology, Stockholm, Sweden

73rd Gaseous Electronics Conference, Virtual Conference,
October 5, 2020

Introduction

- The various plasma surface interaction processes have a significant influence on discharge properties
- In discharge modeling these processes are commonly described by parameters that give the probability of occurrence of the process such as
  - surface recombination to form molecules
  - surface quenching of metastable states
  - electron emission from surfaces due to ion, electron and neutral bombardment of surfaces
  - species reflection from surfaces
  - sputter yields due to ion bombardment
  - surface sticking probabilities for atoms and molecules
- The surface interaction parameters, often describe a complex processes, that are not well understood, by a single number

Introduction

- These parameters depend on surface temperature, surface type as well as the discharge properties
- Emission of secondary electrons can result from bombardment of electrons, ions or neutrals on a surface
- The yield γ_{see} is defined as the number of secondary electrons emitted per incident species
- The surface recombination probability γ_{F} of fluorine atoms on various surfaces at 300 and 80 K

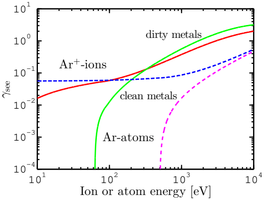

Phelps et al. PSST **8** R21 and PSST **8** B1

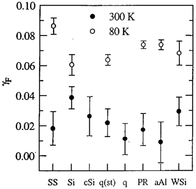

Kota et al. (1999) JVSTA **17** 282

Outline

- 1. Atom surface recombination
    - 1.1. Inductively coupled oxygen discharge
    - 1.2. Inductively coupled chlorine discharge
- 2. Surface quenching of metastable molecules
    - Capacitively coupled oxygen discharge
- 3. Sputter yield
    - Reactive high power impulse magnetron sputtering (HiPIMS)

1. Atom surface recombination

A global (volume averaged) model study

The global (volume averaged) model

- The wall recombination coefficient $\gamma_{\rm rec}$ is one of the most important parameters in molecular discharge modelling
- In the global model the diffusional losses of neutral atoms to the reactor walls are given by

$$k_{\rm atom,wall} = \left[\frac{\Lambda_{\rm atom}^2}{D_{\rm atom}} + \frac{2V(2-\gamma_{\rm rec})}{A v_{\rm atom}\gamma_{\rm rec}} \right]^{-1} \quad {\rm s}^{-1}$$

  - $D_{\rm atom}$ is the diffusion coefficient for neutral atoms
  - $v_{\rm atom} = (8eT_{\rm g}/\pi m_{\rm atom})^{1/2}$ is the mean atom velocity
  - $\gamma_{\rm rec}$ is the wall recombination coefficient for neutral atoms on the wall surface
  - $\Lambda_{\rm atom}$ is the effective diffusion length of neutral atoms

$$\Lambda_{\rm atom} = \left[\left(\frac{\pi}{L}\right)^2 + \left(\frac{2.405}{R}\right)^2 \right]^{-1/2}$$

1.1. Inductively coupled Oxygen discharge

Surface recombination

- The pressure dependence on the wall recombination coefficient was achieved by fitting all the available data for stainless steel surfaces
- For anodized aluminium reactor walls the recombination coefficient is assumed to be a constant $\gamma_{\rm rec} = 0.06$ (Guha et al., 2008)
- The same wall recombination coefficient was used for $O(^1D)$ as no data is available

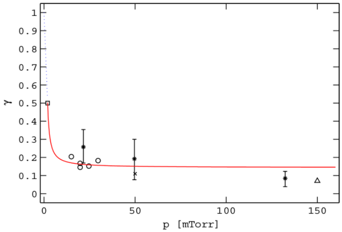

Figure 1. The recombination coefficient of oxygen atoms at the chamber walls for stainless steel as a function of pressure. The measured data is taken from, o Singh *et al* [47], × Matsushita *et al* [90], △ Mozetič and Zalar [91], ☐ Booth and Sadeghi [44] and ∗ Gomez *et al* [46]. The solid line shows a fit to the measured data and the dotted line is a linear extrapolation from $\gamma = 0.5$ at 2 mTorr to $\gamma = 1.0$ at vacuum.

The wall recombination coefficient for oxygen atoms on stainless steel surfaces depends on pressure through

$$\gamma_{\rm rec} = 0.1438 \exp(2.5069/p) \quad p > 2\ {\rm mTorr}$$

$$\gamma_{\rm rec} = -0.25p + 1 \quad p < 2\ {\rm mTorr}$$

Gudmundsson and Thorsteinsson (2007) PSST **16** 399

Particle densities

- The dominant species is the oxygen molecule in the ground state $O_2(X^3\Sigma_g)$ followed by the oxygen atom in the ground state $O(^3P)$
- The singlet metastable states $O_2(a^1\Delta_g)$ and $O_2(b^1\Sigma_g^+)$ and the metastable atom $O(^1D)$ are also present in the plasma in significant amounts
- a cylindrical stainless steel chamber

radius $R = 15$ cm and length $L = 30$ cm $P_{\rm abs} = 500$ W

Toneli et al. (2015a) J. Phys. D **48** 325202

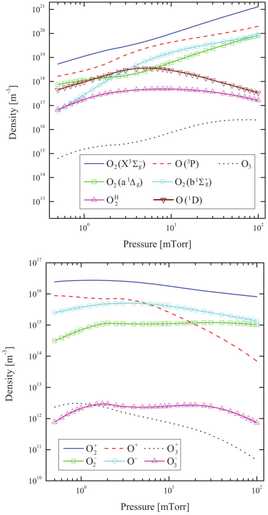

Influence of chamber wall and EEDF

- The chamber wall has a significant influence on the dissociation fraction
    - the dissociation fraction is much higher for anodized aluminium reactor walls
- The parameter *x* defines the shape of the electron energy distribution
    - $x = 0.5$ is concave or bi-Maxwellian
    - $x = 1$ is Maxwellian distribution
    - $x = 2$ is Druyvesteyn distribution

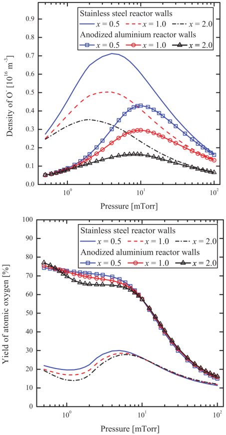

Toneli et al. (2015b) J. Phys. D **48** 495203

1.2. Inductively coupled Chlorine discharge

Surface recombination

- Chlorine is widely used in plasma etching of both semiconductors and metals and chlorine atoms are believed to be the primary reactant
- The dissociation fraction and electronegativity versus the surface recombination of atomic chlorine
- For a large $\gamma_{\rm rec}$, the fractional dissociation decreases
- For the $\gamma_{\rm rec} = 0.1$ the chlorine discharge is 80 % dissociated
- The negative ion density exceeds the electron density at $\gamma_{\rm rec} = 0.08$ at a pressure of 100 mTorr

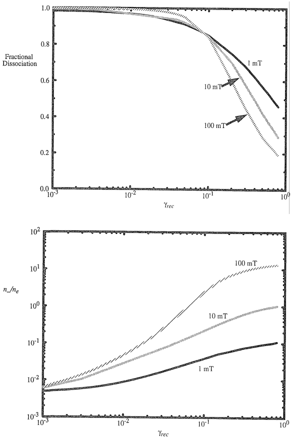

Lee and Lieberman (1995) JVSTA **13** 368

Surface recombination

- The wall recombination probability, $\gamma_{\rm rec}$, is a very important quantity in all low pressure molecular discharges
- We use the wall recombination coefficient measured by Stafford et al. (2009) for stainless steel
- The wall recombination coefficient depends on the dissociation fraction and the wall material

Guha et al. (2008) J. Appl. Phys. **103** 013306

Stafford et al. (2009) J. Phys. D: Appl. Phys. **42** 055206

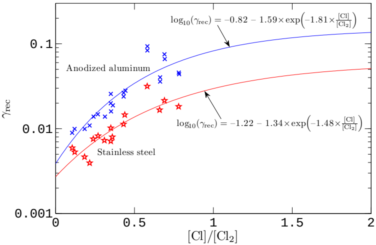

A fit to the measured data is for anodized aluminum

$$\log_{10}(\gamma_{\rm rec}) = -0.82 - 1.59\ \exp\left(-1.81 \times \frac{[\rm Cl]}{[\rm Cl_2]}\right)$$

and for stainless steel

$$\log_{10}(\gamma_{\rm rec}) = -1.22 - 1.34\ \exp\left(-1.48 \times \frac{[\rm Cl]}{[\rm Cl_2]}\right)$$

Gas temperature

- Donnelly and Malyshev (2000) found that the neutral chlorine gas temperature was between 300 and 1250 K, increasing with power and pressure up to 1000 W and 20 mTorr

Donnelly and Malyshev (2000) Appl. Phys. Lett. **77** 2467

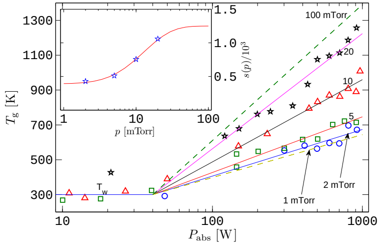

A fit through the measured data gives

$$T_g(P_{abs}, p) = 300 + s(p)\frac{\log_{10}(P_{abs}/40)}{\log_{10}(40)}$$

where

$$s(p) = 1250\,(1 - e^{-0.091\times p}) + 400\,e^{-0.337\times p}$$

Comparison with experiments

- Densities of neutral Cl atoms and electrons versus power
- The agreement with the measured electron density is excellent
- The calculated density of atomic chlorine is in a very good agreement with the measured data at both 1 and 10 mTorr

Malyshev and Donnelly (2000) J. Appl. Phys. **88** 6207

Malyshev and Donnelly (2001) J. Appl. Phys. **90** 1130

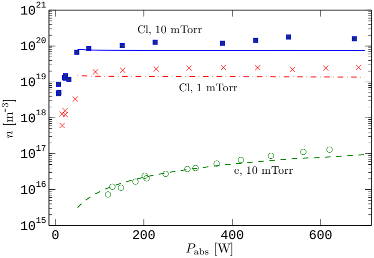

- inductively coupled cylindrical stainless steel chamber
- $L = 20$ cm and $R = 18.5$ cm

Thorsteinsson and Gudmundsson (2010a) Plasma Sources Sci. Technol. **19** 015001

Dilution with oxygen

- When the chlorine discharge is diluted by oxygen chlorine-oxide molecules, such as ClO or ClO_2 are formed at surfaces
- The desorbing flux of ClO_2 was found to be significantly smaller than that of ClO molecules
- The wall recombination coefficient for ClO production was determined by subtracting the Cl_2 production from the total Cl wall recombination coefficient

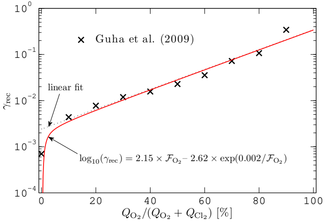

Thorsteinsson and Gudmundsson (2010b)

Plasma Sources Sci. Technol. **19** 055008

Particle densities

- The total rate for creation and loss of ClO molecules is at maximum when the oxygen content is 65%
- Wall recombination of Cl molecules, is the dominating pathway for creation of ClO molecules
- The bulk processes and recombination of ClO^+ ions at the wall account for roughly 33–43% of the total rate for ClO creation, combined

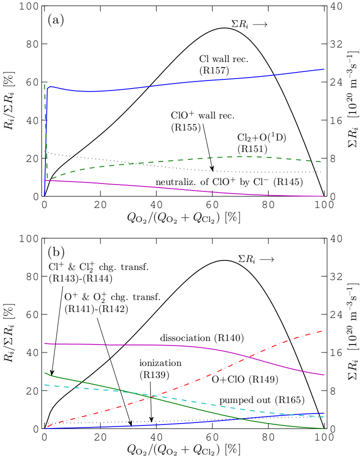

Thorsteinsson and Gudmundsson (2010b) PSST **19** 055008

2. Surface quenching of metastable molecules

Capacitively Coupled Oxygen Discharge

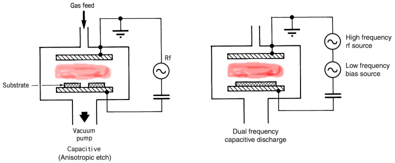

Lieberman and Lichtenberg (2005) *Principles of Plasma Discharges and Materials Processing*, John Wiley & Sons

- A 1D particle-in-cell/Monte Carlo collision simulation
  - Oxygen discharge
  - Capacitively Coupled Oxygen Discharge at 13.56 MHz
    - surface quenching of $O_2(a^1\Delta_g)$
    - the effect of $\gamma_{\rm see}(\mathcal{E})$
- We use the `oopd1` (objective oriented plasma device for one dimension) code to simulate the discharge
- The discharge model includes energy dependent secondary electron emission yield

Gudmundsson et al. *Plasma Sources Sci. Technol.* **22** 035011 (2013)

Oxygen CCP – pressure dependence

- We apply a voltage source with a single frequency

$$V(t) = V_{\mathrm{rf}} \sin(2\pi f t)$$

- The electrodes are circular with a diameter of 14.36 cm
- The gap between the electrodes is 4.5 cm
- We set V_{rf} = 222 V and f = 13.56 MHz
- The neutrals (O_2 and O) are treated as background gas at T_{g} = 300 K with a Maxwellian distribution
- The dissociation fraction and the metastable fraction is found using a global model
- The pressure is varied from 10 – 50 mTorr

Oxygen CCP – surface quenching of $O_2(a^1\Delta_g)$

- At 10 mTorr almost all the electron heating occurs in the plasma bulk (the electronegative core) and the electron heating profile is independent of the surface quenching coefficient
- At 50 mTorr only for the highest surface quenching coefficients 0.1 and 0.01 there is some electron heating observed in the bulk region
- Typical value is 0.007 for iron (Sharpless and Slanger, 1989)

Proto and Gudmundsson (2018b) PSST **27** 074002

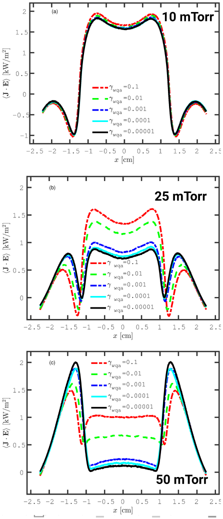

Oxygen CCP – surface quenching of $O_2(a^1\Delta_g)$

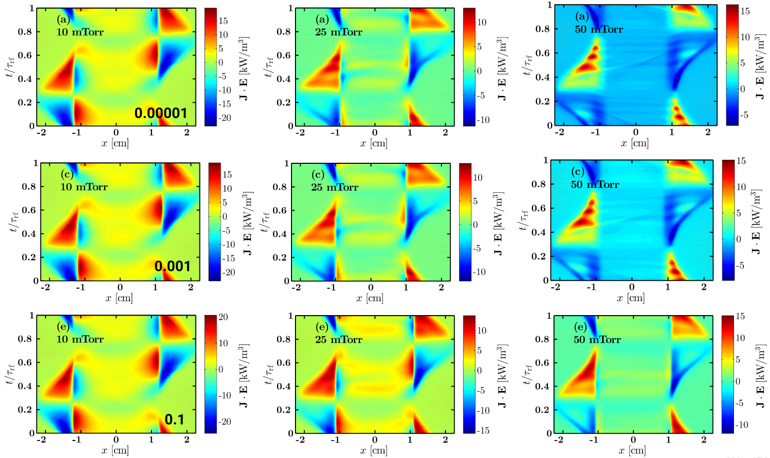

Proto and Gudmundsson (2018b) PSST **27** 074002

The oxygen discharge

- The discharge model also includes energy dependent secondary electron emission yield
- We have compiled experimental data from the literature on secondary electron emission yields for the species O_2^+, O^+, O_2 and O bombarding various metals and substances
- A fit was made through the available experimental data

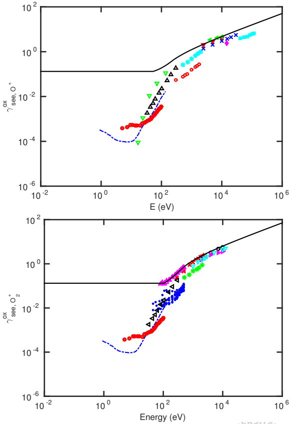

Hannesdottir and Gudmundsson (2016) PSST **25** 055002

Oxygen CCP – the effect of $\gamma_{\rm see}(E)$

- Adding secondary electron emission yield
  - increases the electron density
  - increases the electron heating rate in the sheath region
  - the sheath region becomes narrower
  - a high energy tail appears in the EEPF

Hannesdottir and Gudmundsson PSST **25** 055002 (2016)

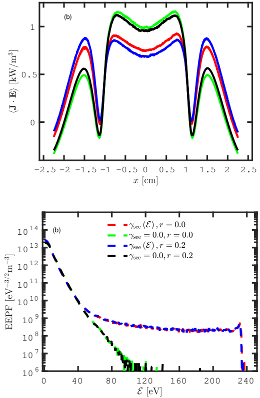

Oxygen at 25 mTorr

Proto and Gudmundsson (2018a) Atoms **6**(4) 65

Oxygen CCP – the effect of $\gamma_{\text{see}}(E)$

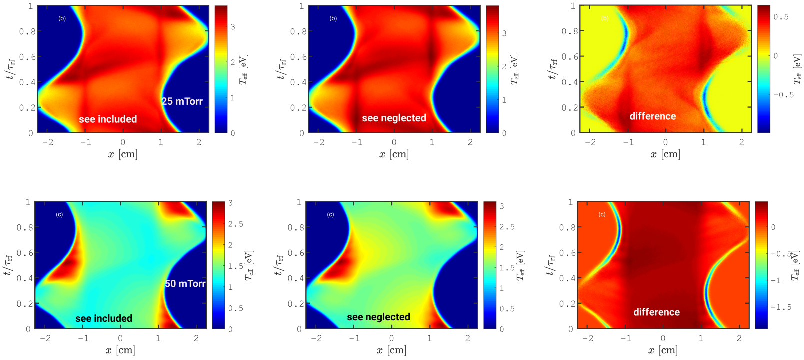

Proto and Gudmundsson (2018a) Atoms **6**(4) 65

- Including secondary electron emission increases the electron energy and decreases the electron power absorption

3. Sputter yield

Reactive high power impulse magnetron sputtering (HiPIMS)

Magnetron sputtering discharges

- Magnetron sputtering discharges are widely used in thin film deposition
- In a dcMS the power density (plasma density) is limited by the thermal load on the target
- High ionization of sputtered material requires very high density plasma
- In a HiPIMS discharge a high power pulse is supplied for a short period
  - low frequency
  - low duty cycle
  - low average power

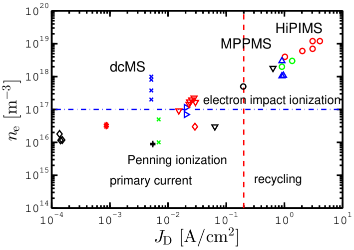

From Gudmundsson (2020) PSST **29** in press

HiPIMS - Voltage - Current - time

- During **reactive sputtering**, a reactive gas is added to the inert working gas and a transition to oxide mode is observed
- The Ar/O_2 discharge with titanium target
- The current waveform is highly dependent on the repetition frequency and applied voltage which is linked to oxide formation on the target
- The current is found to increase significantly as the frequency is lowered

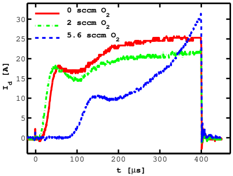

Gudmundsson (2016) PPCF **58** 014002

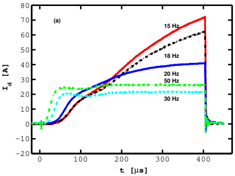

Magnus et al. (2012) JVSTA **30** 050601

Ionization region model studies of reactive HiPIMS

- The ionization region model (IRM) was developed to improve the understanding of the plasma behaviour during a HiPIMS pulse and the afterglow
- It is a time dependent global model of the plasma chemistry of the ionization region (IR) is defined next to the race track
- The IR is defined as an annular cylinder with outer radii r_{c2}, inner radii r_{c1} and length $L = z_2 - z_1$, extends from z_1 to z_2 axially away from the target

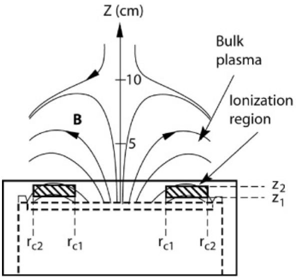

The definition of the volume covered by the IRM

From Raadu et al. (2011) PSST **20** 065007

Ionization region model studies of reactive HiPIMS

- The sputter yield for the various bombarding ions was calculated by TRIDYN for
  - **Metal mode** – Ti target
  - **Poisoned mode** – TiO_2 target
- The yields correspond to the extreme cases of either clean Ti surface and a surface completely oxidized (TiO_2 surface)
- The sputter yield is much lower for poisoned target

The sputter yield data is from Tomáš Kubart, Uppsala University

(a)

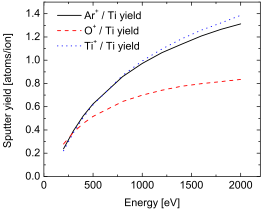

(b)

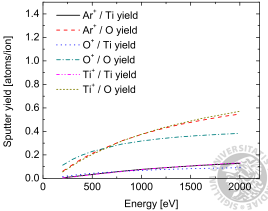

Ionization region model studies of reactive HiPIMS

- Ar^+ and Ti^+-ions contribute most significantly to the discharge current at the cathode target surface – almost equal contribution

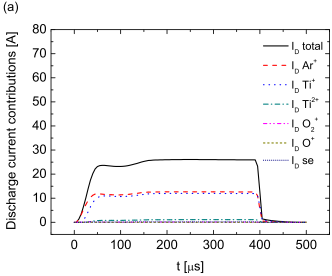

The temporal evolution of the neutral species with **5 % oxygen partial flow** rate for Ar/O_2 discharge with Ti target in **metal mode**.

Gudmundsson et al. (2016) PSST 25(6) 065004

Ionization region model studies of reactive HiPIMS

- Ar^+ contribute most significantly to the discharge current – almost solely – at the cathode target surface
- The contribution of secondary electron emission is very small

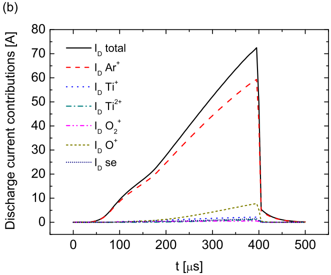

The temporal evolution of the neutral species with **5 % oxygen partial flow** rate for Ar/O_2 discharge with Ti target in **poisoned mode**.

Gudmundsson et al. (2016) PSST 25(6) 065004

Ionization region model studies of reactive HiPIMS

- The increase in the atomic oxygen in the ground state is due to:
  - sputtering of O(^{3}P) from the partially to fully oxidized target (dominates)
  - electron impact de-excitation of O(^{1}D)
  - electron impact dissociation of the O$_2$ ground state molecule

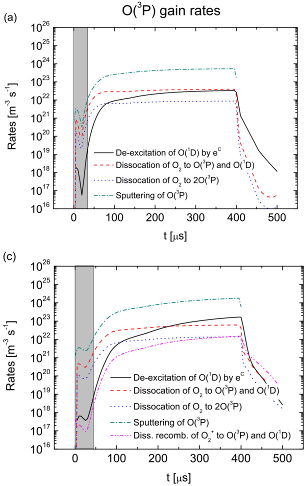

The temporal evolution of the neutral species with **5 % oxygen partial flow** rate for Ar/O$_2$ discharge with Ti target in **transition mode** and **poisoned mode**.

Lundin et al. (2017) JAP 121(17) 171917

Summary

Summary

- The importance of surface processes has been demonstrated by a few examples
    - Surface recombination of atoms dictates the dissociation fraction in inductively coupled discharge
    - Surface quenching of molecular metastables dictates the electronegativity and electron power absorption mechansim in a capacitively coupled oxygen discharge
    - The sutter yield determines the dominating ion in a reactive HiPIMS discharge and therefore the dominating the recycling process
- In discharge modeling it is important to include a carefully selected surface process parameters

Acknowledgements

Thank you for your attention

The slides can be downloaded at

`http://langmuir.raunvis.hi.is/~tumi/ranns.html`

References

Donnelly, V. M. and M. V. Malyshev (2000). Diagnostics of inductively coupled chlorine plasmas: Measurements of the neutral gas temperature. *Applied Physics Letters 77*(16), 2467–2469.

Gudmundsson, J. T. (2016). On reactive high power impulse magnetron sputtering. *Plasma Physics and Controlled Fusion 58*(1), 014002.

Gudmundsson, J. T. (2020). Physics and technology of magnetron sputtering discharges. *Plasma Sources Science and Technology 29* in press.

Gudmundsson, J. T. and D. Lundin (2020). Introduction to magnetron sputtering. In D. Lundin, T. Minea, and J. T. Gudmundsson (Eds.), *High Power Impulse Mangetron Sputtering: Fundamentals, Technologies, Challenges and Applications*, pp. 1–48. Amsterdam, The Netherlands: Elsevier.

Gudmundsson, J. T., D. Lundin, N. Brenning, M. A. Raadu, C. Huo, and T. M. Minea (2016). An ionization region model of the reactive Ar/O_2 high power impulse magnetron sputtering discharge. *Plasma Sources Science and Technology 25*(6), 065004.

Gudmundsson, J. T., F. Magnus, T. K. Tryggvason, S. Shayestehaminzadeh, O. B. Sveinsson, and S. Olafsson (2013). Reactive high power impulse magnetron sputtering. In *Proceedings of the XII International Symposium on Sputtering and Plasma Processes (ISSP 2013)*, pp. 192–194.

Gudmundsson, J. T. and E. G. Thorsteinsson (2007). Oxygen discharges diluted with argon: dissociation processes. *Plasma Sources Science and Technology 16*(2), 399–412.

Guha, J., V. M. Donnelly, and Y.-K. Pu (2008). Mass and Auger electron spectroscopy studies of the interactions of atomic and molecular chlorine on a plasma reactor wall. *Journal of Applied Physics 103*(1), 013306.

Hannesdottir, H. and J. T. Gudmundsson (2016). The role of the metastable $O_2(b^1\Sigma_g^+)$ and energy-dependent secondary electron emission yields in capacitively coupled oxygen discharges. *Plasma Sources Science and Technology 25*(5), 055002.

References

Kim, S., M. A. Lieberman, A. J. Lichtenberg, and J. T. Gudmundsson (2006). Improved volume-averaged model for steady and pulsed-power electronegative discharges. *Journal of Vacuum Science and Technology A 24*(6), 2025–2040.

Kota, G. P., J. W. Coburn, and D. B. Graves (1999). Heterogeneous recombination of atomic bromine and fluorine. *Journal of Vacuum Science and Technology A 17*(1), 282–290.

Lee, C. and M. A. Lieberman (1995). Global model of Ar, O_2, Cl_2 and Ar/O_2 high-density plasma discharges. *Journal of Vacuum Science and Technology A 13*(2), 368–380.

Lieberman, M. A. and A. J. Lichtenberg (2005). *Principles of Plasma Discharges and Materials Processing* (2 ed.). New York: John Wiley & Sons.

Lundin, D., J. T. Gudmundsson, N. Brenning, M. A. Raadu, and T. M. Minea (2017). A study of the oxygen dynamics in a reactive Ar/O_2 high power impulse magnetron sputtering discharge using an ionization region model. *Journal of Applied Physics 121*(17), 171917.

Magnus, F., T. K. Tryggvason, S. Olafsson, and J. T. Gudmundsson (2012). Current-voltage-time characteristics of the reactive Ar/O_2 high power impulse magnetron sputtering discharge. *Journal of Vacuum Science and Technology A 30*(5), 050601.

Malyshev, M. V. and V. M. Donnelly (2000). Diagnostics of inductively coupled chlorine plasmas: Measurement of Cl_2 and Cl number densities. *Journal of Applied Physics 88*(11), 6207 – 6215.

Malyshev, M. V. and V. M. Donnelly (2001). Diagnostics of inductively coupled chlorine plasmas: Measurement of electron and total positive ion densities. *Journal of Applied Physics 90*(3), 1130–1137.

Phelps, A. V. and Z. L. Petrović (1999). Cold-cathode discharges and breakdown in argon: surface and gas phase production of secondary electrons. *Plasma Sources Science and Technology 8*(3), R21–R44.

Phelps, A. V., L. C. Pitchford, C. Pédoussat, and Z. Donkó (1999). Use of secondary-electron yields determined from breakdown data in cathode-fall models for Ar. *Plasma Sources Science and Technology 8*(4), B1–B2.

References

Proto, A. and J. T. Gudmundsson (2018a). The influence of secondary electron emission and electron reflection on a capacitively coupled oxygen discharge. *Atoms 6*(4), 65.

Proto, A. and J. T. Gudmundsson (2018b). The role of surface quenching of the singlet delta molecule in a capacitively coupled oxygen discharge. *Plasma Sources Science and Technology 27*(7), 074002.

Raadu, M. A., I. Axnäs, J. T. Gudmundsson, C. Huo, and N. Brenning (2011). An ionization region model for high power impulse magnetron sputtering discharges. *Plasma Sources Science and Technology 20*(6), 065007.

Sharpless, R. L. and T. G. Slanger (1989). Surface chemistry of metastable oxygen. II. Destruction of $O_2(a^1\Delta_g)$. *Journal of Chemical Physics 91*(12), 7947 – 7950.

Stafford, L., R. Khare, J. Guha, V. M. Donnelly, J.-S. Poirier, and J. Margot (2009). Recombination of chlorine atoms on plasma-conditioned stainless steel surfaces in the presence of adsorbed Cl_2. *Journal of Physics D: Applied Physics 42*(5), 055206.

Thorsteinsson, E. G. and J. T. Gudmundsson (2010a). A global (volume averaged) model of a chlorine discharge. *Plasma Sources Science and Technology 19*(1), 015001.

Thorsteinsson, E. G. and J. T. Gudmundsson (2010b). The low pressure Cl_2/O_2 discharge and the role of ClO. *Plasma Sources Science and Technology 19*(5), 055008.

Toneli, D. A., R. S. Pessoa, M. Roberto, and J. T. Gudmundsson (2015a). On the formation and annihilation of the singlet molecular metastables in an oxygen discharge. *Journal of Physics D: Applied Physics 48*(32), 325202.

Toneli, D. A., R. S. Pessoa, M. Roberto, and J. T. Gudmundsson (2015b). A volume averaged global model study of the influence of the electron energy distribution and the wall material on an oxygen discharge. *Journal of Physics D: Applied Physics 48*(49), 495203.